Article:
Li, J., Wei, J., Chen, H. et al. (3 more authors) (2025) Study on the combustion and emission characteristics of a compression ignition engine using diesel/ethanol blend with carbon nanoadditives. Renewable Energy, 246. 122941. ISSN 0960-1481

https://doi.org/10.1016/j.renene.2025.122941

Study on the combustion and emission characteristics of a compression ignition engine using diesel/ethanol blend with carbon nanoadditives

Abstract: This article focuses on the effects of adding different types (graphene oxides, multi-layered graphene oxides, multi-walled carbon nanotubes) and dosages (25ppm, 100ppm) of renewable carbon nanoparticles to the diesel/ethanol blend towards the combustion and emission characteristics of a compression-ignition engine. The research showed that a shortened ignition delay was brought about due to the presence of carbon nanoparticles, with the most pronounced effect achieved by multi-walled carbon nanotubes. Regarding in-cylinder combustion, the inclusion of carbon nanoparticles induced an enhancement to the combustion progress, associated with increments in peak cylinder gas pressure and peak heat release rate and a decrement in combustion duration, most notably accomplished by graphene oxides. Moreover, the engine exhibits lower fuel consumption and better fuel utilization based on the carbon nanoparticles addition, where the nano-fuels with graphene oxides possess the minimum brake specific fuel consumption and maximum brake thermal efficiency. Concerning the abatement effect, by applying carbon nanoparticles, emissions of CO, HC and soot were decreased by 37.95%, 45.18% and 47.83%, respectively, however, a slight increase in NOx emissions also occurred. In particular, multi-walled carbon nanotubes offered the most significant mitigations in CO and HC, while graphene oxides achieved the greatest abatement in soot emissions.

Keywords**:** Diesel engines, Renewable Carbon nanoadditives, Renewable Ethanol, Combustion, Performance, Emissions

1. Introduction

In recent years, accompanied by tremendous economic expansion and explosive technological evolution, fossil energy scarcity has become a serious worldwide crisis. Against this backdrop, renewable energy sources are gradually becoming an overwhelming substitute for non-renewable energy sources. As one of the most widely used energy conversion devices in agricultural machinery and power generation [1, 2], diesel engines are characterized by high thermal efficiency, high reliability and low maintenance costs. At present, a variety of innovative technologies have been employed to enable the efficient and clean combustion of diesel, specifically combustion improvement [3, 4] and engine design modification [5]. Among the techniques, combustion improvement is undoubtedly desirable as it has the minimum complication implicated, which could be attained through optimizing fuel properties and improving injection strategies. Therefore, in the broad backdrop to the rapid take-off of renewable energies, the employment of renewable and clean alternative fuels in diesel engines presents an essential approach. Alcohol-based alternative fuels, widely recognized for their nature to enhance fuel combustion, have been recently advocated for application in commercial vehicles by the policies of many countries and agencies [6, 7]. Among these, available from sugar in vegetables through alcoholic fermentation [8], ethanol, as a renewable biomass-based alternative fuel, has gained the interest of many researchers. With a high octane number, ethanol is widely incorporated into gasoline to obtain increased torque for spark-ignition engines without any knock [9, 10]. In terms of diesel engines, however, the lower viscosity and cetane number of ethanol prevents it from igniting without auxiliary ignition, which could be mitigated by blending with diesel fuel. While the cylinder co-combustion from diesel fuel and ethanol is available through direct mixing [11] or double-jet design [12, 13], as no engine modification is required, direct mixing is clearly a more affordable way.

According to previous experimental studies [14, 15], used as a diesel fuel additive, ethanol was found to accelerate the combustion process and minimize soot emission. However, the fuel evaporation difficulty and energy content deprivation create obstacles to further utilization as a diesel alternative. The research conducted by Rakopoulos et al. [8] reported an increased ignition delay due to the low cetane number of ethanol. Furthermore, Kumar et al. [16] noticed that the inclusion of ethanol lowered the calorific value of the fuel, which elevated the brake specific fuel consumption (BSFC). Moreover, based on the cooling effect and prolonged ignition delay formed by the low cetane number and calorific value of ethanol, such issues as increased HC and CO emissions were revealed to arise with the presence of ethanol [14, 17]. Confronting the problems shared by such alcohol substitution fuels, in the investigation conducted by Chen et al. [18], the adjustment in the fuel injection timing has been adopted. However, their results indicated that the injection timing, once adjusted, was found to cause an increase in either NOx emissions or soot emissions, probably not an unquestionably absolute abatement strategy.

In recent years, supported by advances in nanotechnology, experimental works around the application of nano-fuel additives have come to the forefront. As many studies reported, the introduction of nanoparticles has been proven to shorten the ignition delay and improve the fuel economy, together with decreasing emissions. The research carried out by Simhadri et al. [19] focused on the impacts of TiO_2 on the engine fueled with diesel fuel containing 20%vol Mahua biodiesel under various injection pressures. The results indicated that TiO_2 nanoparticles effectively improved the ignition quality and the fuel economy, especially at low injection pressure. Besides, their emissions were also significantly reduced, with decrements by 31.5%, 38.5%, 9.1% and 5.5% in CO, HC, smoke opacity and NOx. These could be ascribed to the favorable assets of nanoparticles, including

evaporation acceleration [20], combustion enhancement [21] and fuel distribution improvement (strengthened micro-explosion [22]), which is associated with the high specific area and high thermal conductivity of nanoparticles. Comprised of metals with high thermal conductivity, metallic nanomaterials have demonstrated desirable enhancements upon engine combustion and emissions in previous studies as a fuel additive. Rajesh et al. [23] revealed increments in peak in-cylinder pressure and peak heat release rate by 8.82% and 16.4%, respectively, upon the incorporation of alumina nanoparticles into biodiesel, coupled with reductions in combustion duration and ignition delay. They interpreted the efficacy of the nano-additives in terms of the catalytic behavior of the nanoparticles that accelerated the combustion rate. Besides, the addition of metal nanoparticles cut down the emissions in CO, HC and smoke, yet for the most part, they present remarkable compensation above NOx. As an example, in the experiment conducted by Rejish et al. [23], the inclusion of alumina particles obtained reductions in the ranges of 25%-33.3% and 19.4%-26.5% in CO and HC, respectively, and NOx was increased in the range of 118.2%-23.5%. In addition, during the employment as fuel additives for metallic nanomaterials, the exhaust gas from the combustion would contain the metal residual as the metal particles couldn't burn up in the cylinder, which would pose a hazard to human beings and the environment [24]. Consequently, although the effect of metal nanoparticles as fuel additives is absolutely favorable, the application of the fuels with the addition of metal nanoparticles requires further development and cautious consideration in view of the fact that they can exacerbate the toxicity of vehicle exhaust. Therefore, given the growing scarcity of fossil fuels, in order to promote the wide application of ethanol fuels, an environment-friendly nano-additive without introducing new impurities into engine exhaust is expected.

Carbon-based nanomaterials, as renewable materials, can be prepared by pyrolysis or salt-based

methods from agricultural/agro-industrial wastes and municipal wastes [25, 26]. Importantly, carbon-based nanoparticles are structured by carbon atoms, hence their utilization as fuel additives is less toxic than metal nanoparticles. Moreover, compared with metal nanoparticles, carbon nanoparticles are less prone to form aggregation since there is less magnetic attraction between nanoparticles [27]. Besides, carbon nanoparticles are reported to exhibit superior mechanical stretchability/ flexibility and carrier mobility, efficiently improving the anti-friction properties of the mechanical components, especially for carbon nanotubes (CNT) [28, 29] and graphene [30, 31]. Kaleli and Demirtas [32] studied the tribological properties of a synthetic engine with the incorporation of redox graphene oxide. The results showed that the utilization of the redox graphite oxide minimized the friction coefficient of the ball on the polished cylinder liner by 3.29%. Moreover, carbon-based nanomaterials simultaneously benefited the combustion progress and the tribological characteristics, which is of great significance in the improvement of fuel economy. Chacko and Jeyaseelan [21] studied the influence of graphene-based fuel additives upon the combustion and emission behavior in a turbocharged diesel engine, where a decrement of 5.5% in BSFC and an increment of 1.4% over brake thermal efficiency (BTE) were observed. Similarly, within our prior investigation, graphene oxide and CNTs led to considerable fuel utilization enhancement upon incorporation into the methanol/diesel blends, with BSFC reduced by 1.7% and BTE increased by 4.8% [33]. In the study conducted by Selvan et al. [34] focused on the characteristics of the engine fueled in diesel-ethanol-biodiesel blends adding nano-additives containing a combination of cerium oxide nanoparticles and CNT. The results of the study pointed out that the combined effect of CNT and cerium oxide resulted in enhanced fuel economy, accompanied by a 7.7% decrease on BSFC and a 7.5% increase on BTE. What's more, many studies have focused on the comparative analysis of carbon nanomaterials and metal nanomaterials, where the relative

prominence of carbon nanomaterials for abatement is revealed. Ooi et al. [35] conducted a comparative study for single-walled carbon nanotubes, cerium oxide and graphene oxide, discovering that single-walled carbon nanotubes provided maximum benefits in terms of combustion and emissions, along with reductions of 10.3%, 14.6%, 23.4% and 24.1% in ignition delay, combustion duration and CO, HC emissions, respectively. The impacts of carbon nanoparticles and Ag nanoparticles on the combustion parameters of the engine were investigated comparatively in the study conducted by Najafi [36]. Compared with the nanofuels with Ag nanoparticles, the nanofuels with CNT offered lower BSFC and CO emissions, yet marginally higher HC emissions. In the study conducted by Mei et al. [37], CNT has demonstrated a more pronounced improvement in ignition quality and emission reduction (HC, CO, smoke, NOx) in comparison with MoO_3. Maniganda et al. [38] explored the effect of TiO_2, CNT, Al_2O_3, CuO, CeO_2 and hydrogen blends on the combustion, performance and emission characteristics of the dual-fuel engine. The maximum reduction in CO was achieved by TiO_2, while the minimum emissions in HC and NOx were obtained for CNT, with decrements of 90% and 33%, respectively. It can be seen that compared to metallic nanomaterials, although it is debatable whether carbon nanomaterials possess absolutely more outstanding capability in emission reduction, carbon nanomaterials are firmly proven to cause minor NOx discharge, which is definitely conducive to the mitigation of environmental pollution issues. In addition, carbon-based nanomaterials are acknowledged to offer significant industrial enhancements, including removing dyes from wastewater [39], improving the performance of epoxy composites [40] and modifying glassy carbon electrodes [41]. These industrial requirements have stimulated continuous technological renewal in the manufacturing of carbon-based nanomaterials. Though their price is currently high due to the complications in the production process [42], there is a tendency for it to diminish over time, and

carbon nanomaterials are expected to be more of a cost-effective alternative to costly metallic materials and thus are more likely to be widely used as fuel additives in the future.

Ethanol, as a renewable diesel substitution, is capable of reducing in-cylinder incomplete combustion and soot emissions, whereas the high latent heat value (LHV) and low calorific value of ethanol have also set restrictions on its extensive use. Carbon nanomaterials, featuring their superior environmental benefits over metallic nanoparticles, along with favorable fuel-burn nature, are believed to complement the cooling effect and low fuel energy content of ethanol, while offering further improvement in fuel economy without penalty in terms of harmful emissions. Furthermore, carbon-based nanomaterials and ethanol, served as renewable materials, could be produced from renewable resources by pyrolysis and alcoholic fermentation, respectively, and offer high environmental benefits as a novel renewable fuel additive upon combination with each other. However, the present mechanisms of this new renewable fuel additive contributing to combustion improvement and abatement effect remain immature, thus in-depth studies on the joint impact of carbon-based nanoparticles and ethanol against combustion, performance and emission of the engine is especially critical. This paper focuses on the influence of incorporations of three sorts of carbon nanomaterials (graphene oxides, multi-layered graphene oxides and multi-walled carbon nanotubes) towards the combustion and emission characteristics in the engine fueled with the diesel/ethanol blended fuel to investigate the co-mechanism of ethanol and carbon nanoparticles. The goals of this study are listed below.

1) Comparative analysis of the impacts of diverse carbon nanoparticles on combustion behavior and emissions.

2) Selection of the optimal carbon nanomaterial, nanoparticle concentration and loading

conditions.

3) Evaluation of the joint effect of ethanol and carbon nanoparticles on combustion and emissions characteristics of the engine.

2. Materials and methods

2.1. *Fuel preparation*

The fuels employed in this experiment include diesel, the diesel/ethanol blended fuel and the diesel/ethanol nanofluid fuel. The pure diesel fuel is denoted by D100. The diesel/ethanol blended fuel containing 85 vol% diesel and 15 vol% ethanol is referred to as E15. The diesel/ethanol nanofluid fuel was obtained by adding carbon nanoparticles (CNPs) to the E15 fuel, and it varies in terms of the types (graphene oxides GO, the multi-layered graphene oxides MGO and the multi-walled carbon nanotubes MWCNT) and the dosages (25ppm, 100ppm) of CNPs addition. For example, the diesel/ethanol nanofluid fuel with the graphene oxide (GO) added in a dosage of 25ppm into the E15 fuel was shorted as EGO25. Similarly, the EMGO25 is the E15 fuel with muti-layered graphene oxides (MGO) in 25ppm. The E15 fuel with multi-walled carbon nanotube nanoparticles in a mass fraction of 100ppm was EMWCNT100. The primary properties of CNPs and the physiochemical properties of tested fuels are shown in **Table 1** and **Table 2**, respectively. For the preparation for the diesel/ethanol nanofluids, the ethanol was blended with 2000ppm surfactant triton-X100 (Sigma Aldrich, cat#93426-100mL), and the nanoparticles were incorporated in the mixing process. Afterward, the resulting ethanol nanofluids were added to diesel as fuel additives to obtain the diesel/ethanol nanofluids. The whole process was conducted under the powerful stirring of an electromagnetic mixer (at 3000rev/min for 30 min), followed by an ultrasonication for 30 minutes to prevent the agglomeration of CNPs.

Table 1. The carbon nanoparticle additives specifications

Chemical name	Graphene oxides	Multi-layered graphene oxides	Muti-wall carbon nanotubes
Appearance (color)	Black brown	Black	Black
Purity (%)	95	95	>95
Specific area ($m^2 \cdot g^{-1}$)	5~200	5~150	230~270
The diameter (nm)	1	3.4~8	3~15
The length(μm)	10~50	5~50	3~12
Number of polies	1~2	5~10	8~15
Oxygen content (%)	~45	~8	~0
Thermal conductivity	5000	~3000	3000

Table 2. Physiochemical properties of tested fuels

Properties	D100	Ethanol	EGO25	EGO100	EMGO25	EMGO100	ECNT25	ECNT100
Density (kg/m^3@15℃)	830	803	826.4	827.8	827.3	828.9	827.7	829.5
Viscosity (mm^2/s@40℃)	3.35	1.08	4.016	4.049	4.014	4.047	4.01	4.040
Latent heating value (LHV, kJ/kg)	260	900	--	--	--	--	--	--
Cetane number	50.2	9	46.6	48.4	44.7	47.6	47.1	49.0
Calorific value (MJ/ kg)	42.8	27	41.08	41.44	41.16	41.24	41.12	41.65

2.2. *The experimental engine test*

Tests were performed on a single-cylinder, four-stroke, water-cooled CI engine with the specifications listed in **Table 3**. The engine test bench is presented in **Fig.1**. The engine tests were conducted under a fixed speed of 1200 rpm over a broad range of engine loads, i.e., low (10% and 30%), medium (50%), and high (70% and 90%) loads, correlating to torques of 5, 15, 25, 35, and 45 N·m, respectively. During testing, the timing and pressure of the injection were maintained at 18° before the top dead center (BTDC) and 18MPa, respectively. An eddy current dynamometer (Shenck CW25) is attached to the engine, while a dynamometer controller (MIKE (LUOYAN) HORIZON, CMU3A) is engaged to manage the torque and speed of the engine. In the experiment, the fuel consumption was measured by the flowmeter (Shanghai Diesel Engine Research, FCM-D). The cylinder pressure sensor (AVL GH14D) mounted on the head of the cylinder was employed to obtain the signal related to cylinder pressure. Subsequently, the combustion analyzer (AVL HR-CA-B1)

processed the signal and calculated the instantaneous heat release rate [43]. To minimize the impact of inter-cycle variations, 150 consecutive in-cylinder pressure cycles were employed for the combustion evaluation. The investigation focuses on the emissions of hydrocarbon (HC), nitrogen oxide (NO_X), carbon monoxide (CO) and soot. The first three measurements were performed with a gas analyzer (MEXA-584L, HORIBA) whilst the last one was conducted in an opaque smoke meter (Dismoke 4000, AVL). To ensure the accuracy of the experiment, the calibration of the instruments was carried out before measurements. The resolution and accuracy above experimental apparatus are displayed in **Table 4**. The total experimental error θ_{Exp} can be estimated to be 0.54% by the method as follows [44]:

$$\theta_{Exp} = \sqrt{\theta_{speed}^2 + \theta_{torque}^2 + \theta_{pressure}^2 + \theta_{CO}^2 + \theta_{HC}^2 + \theta_{NOx}^2 + \theta_{smoke}^2}$$

For the formula above, θ_x represents the uncertainty in the measurement of the experimental data x given in **Table 2**. To guarantee a reliable and accurate result of the experimental emissions, all parameters were measured three times under the same conditions to obtain the average value.

Before each test, the preparation of new fuel was just completed. Prior to each fuel renewal, the engine would operate with the new fuel for a period of time until no noticeable fluctuations occurred in engine loads or emissions. Throughout the test period, the temperature of the coolant and the oil were maintained within the range of 80±5℃ and 90±5℃ respectively so as to secure the replicability and comparability of the experiments. Otherwise, monitors of discharge temperatures and lubrication pressures are performed on the testing engine to assure normal operation in the engine. Upon completion of the experiment, the check for residue was conducted inside the fuel tank and pipeline, and no left for nanoparticles was observed.

Table 3. Specifications of the testing engine

Engine specifications	
Engine type	Single cylinder 4-stroke
Bore× Stoke	100mm×115mm

Compression ratio	17.5
Displacement	0.903L
Rated power/speed	12.1 kW/2200 rpm
Maximum toque/speed	58.3 N·m /1760 rpm
Injection nozzle	0.32 mm/4
Nozzle opening pressure	18 MPa
Fuel injection advance	18±1 °CA
Cooling type	Water-cooled
Valve phase	
Intake valve open	12 °CA before TDC
Intake valve closed	38 °CA after BDC
Exhaust valve open	55 °CA before BDC
Exhaust valve closed	12 °CA after TDC

Table 4. Revolution values and accuracy of apparatus

Measurement apparatuses	Resolution	Uncertainties
Dynamometer		
Torque measurement	0.01 N·m	±0.2%
Speed measurement	1 rpm	±0.4%
Cylinder pressure sensor		
Pressure transducer	0.01 MPa	±0.22%
Gas analyzer		
CO measurement	0.01%	<0.1%
NOx measurement	1ppm	<0.1%
THC measurement	2 ppm	<0.1%
Smoke opacity meter		
Smoke Opacity	0.1%	<0.1%

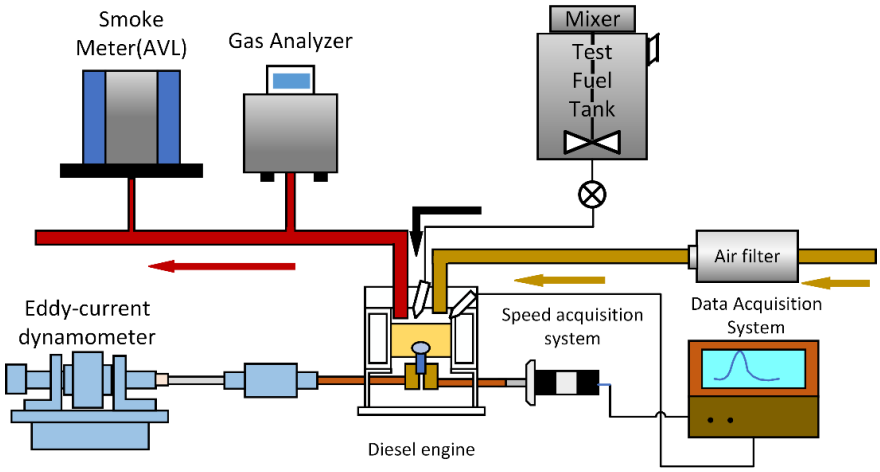

Fig. 1. The work bench of the testing engine

3. Results and discussion

3.1. *Combustion characteristics*

3.1.1. Cylinder gas pressure and heat release rate

Cylinder gas pressure (CGP) and heat release rate (HRR) are the parameters that indicate the combustion behavior, thereby affecting performance and emission behavior in the diesel engine. In the same operating condition, all the tested fuels tend to have the similar trend on the curves of the CGP and HRR against crank angle, while the fuel additives cause measurable impacts on peak CGP and peak HRR, as shown in **Fig.2**, for example. This indicates that the overall combustion quality and premixed combustion quantity, responded to the parameters peak CGP and peak HRR, respectively [45], have been changed due to the presence of fuel additives. The variations in peak CGP and HRR for all fuels with various loading conditions are depicted in **Fig.3 (a) and (b)**.

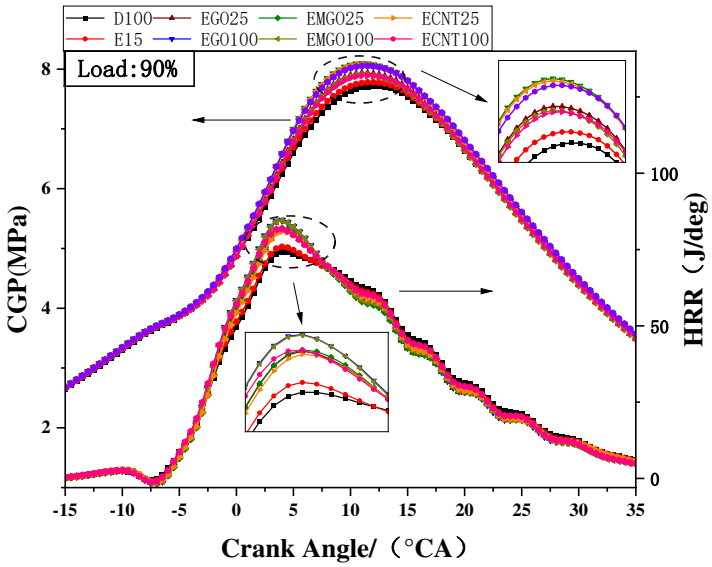

Fig. 2. The diagrams for CGP and HRR against crank angle at 90% of full load

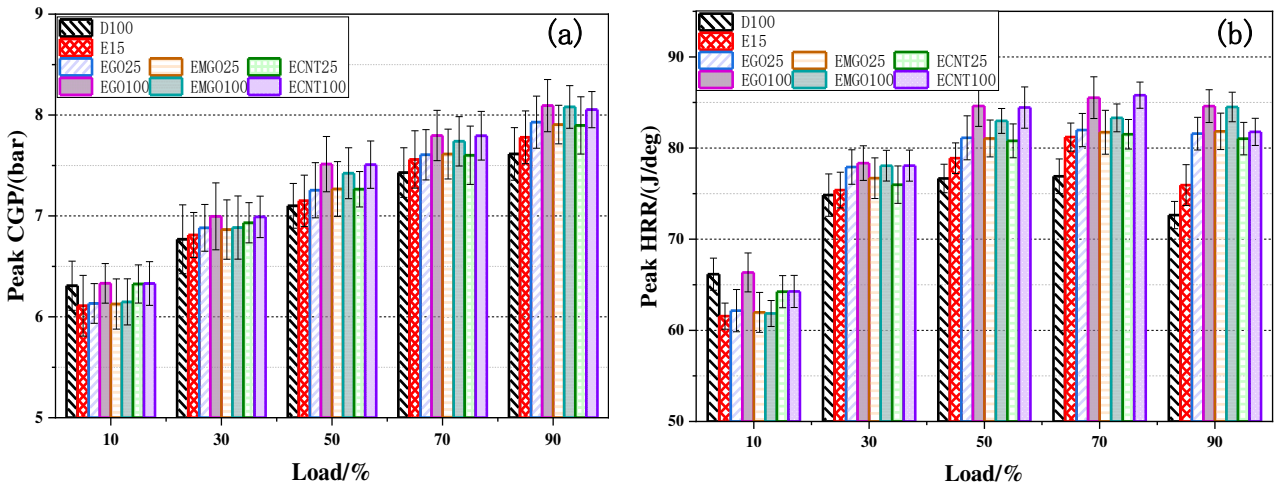

Fig. 3. The diagrams of (a) peak CGP and (b) peak HRR under different loads for all tested fuels.

Fig.3 (a) and (b) depict the variations in peak CGP and HRR for all fuels with various loading conditions. As seen in the figure, after adding the ethanol to diesel, the peak CGP and HRR were decreased at low loads, with a decrement of 3.14% and 6.95% at peak CGP and HRR, respectively. This could be owing to the high latent heat of vaporization (LHV) of ethanol, which caused a drop in cylinder temperature by absorbing a large amount of heat during fuel evaporation under low loads [46]. Furthermore, the blending of ethanol brings about a reduction in cetane number, making it a difficult condition for the ignition of fuel mixture [11]. However, as the load increased, the cooling effect of ethanol was suppressed due to the increased temperature, while the low viscosity and density of ethanol contributed to the well distribution of fuel and the oxygenated nature effectively alleviated the hypoxia phenomenon during combustion, especially at high loads [47, 48]. Therefore, it can be observed a higher peak CGP and HRR for the diesel/ethanol blend compared with diesel, with the maximum increments of 2.16% at peak CGP and 4.52% at peak HRR obtained at 90% load (the largest loading condition).

As observed, for the fuels added with CNPs, i.e. the graphene oxides (GO), the multi-layered graphene oxides (MGO), multi-walled nanotubes (MWCNT), peak CGP and HRR are significantly

higher compared with the diesel/ethanol blend. This is due to the high thermal conductivity and broad specific surface area of CNPs, which enhanced heat transfer and the fuel spray atomization characteristics, leading to a thorough combustion [37, 49]. Furthermore, the surface of CNPs possesses a high activity for energy reactions, which would get pronounced under the high temperature due to more reaction heat provided. This may explain why the maximum increment for CNPs addition is obtained at 90% load. Additionally, with more CNPs added, peak CGP and HRR shows an ascending trend. This is probably attributed to the significant heat sink effect associated with the high concentration of CNPs, which facilitated the heat transfer [50]. According to the results, the peak CGP and HRR increased by 5.08%, 11.4% for EGO100, 3.87%, 11.29% for EMGO100 and 3.52%, 7.69% for EMWCNT100 compared with the diesel/ethanol blend, respectively. It is obvious that the GO possesses the most pronounced improvement for peak CGP and HRR, followed by MGO and MWCNT. The better capability in improving the peak CGP and HRR for GO towards MGO is mainly owing to the fewer layers and smaller size of GO, which brought about a larger specific area and higher fuel oxidation efficiency [51]. The higher peak CGP and HRR for fuels with MGO over that of MWCNT is attributed to the oxygen functional groups of MGO, which increased the combustion rate [21]. This trend is consistent with the similar experiment carried out by Ma et al. [33], who found the improvements on peak CGP and HRR after doping GO nanopowder into the blended fuel (methanol in 10% and diesel in 90%). In detail, they reported that the addition GO elevated the peak CGP and HRR by 5.8% and 13%, respectively, which is higher than the results of this experiment. This is probably because the inclusion of 10% methanol is considered to be able to achieve a smaller viscosity for the fuel compared to 15% ethanol substitution, which reduced the droplet size and increased the fuel-air contact area, favorable for the heat transfer and catalytic effect of the CNPs. In comparison to

diesel, the combined effect of ethanol and CNPs enhances cylinder combustion slightly at low loads, yet considerably at high loads, with maximum enhancements of 6.29% and 16.45% in peak HRR and CGP for EGO100, respectively.

3.1.2 Ignition delay and combustion duration

The ignition delay (ID) for all fuels with a wide range of loading conditions is demonstrated in **Fig.4 (a)**. The ignition delay represents the crank angle period between the start of fuel injection and arrival at 10% burned mass fraction, including two periods i.e. the physical delay period and the chemical delay period, which are influenced by the evaporation and cetane number of the fuel, respectively [52, 53].

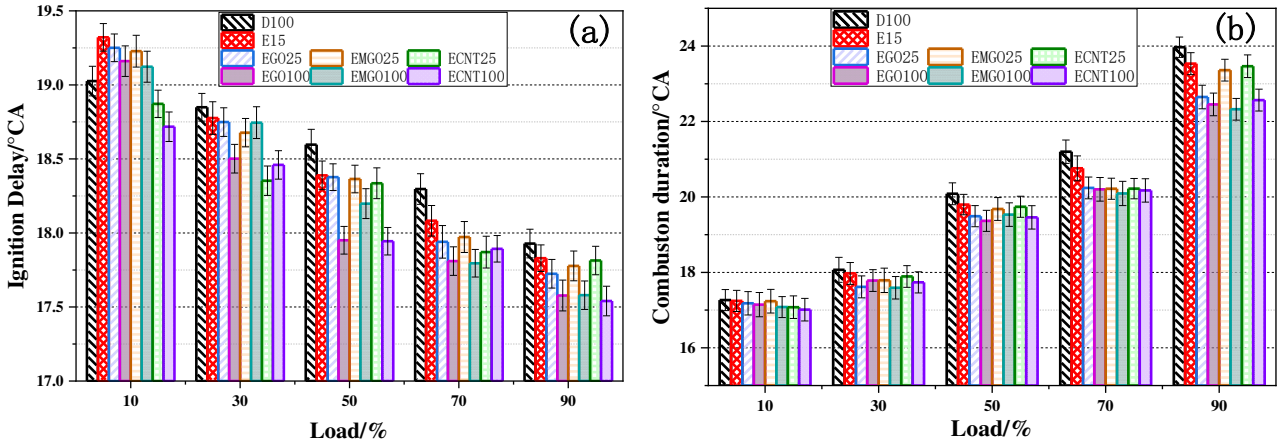

Fig. 4. The diagrams of (a) ID and (b) CD under different loads for all tested fuels.

In the figure, ID presents a decreasing trend with increasing load, which is because the evaporation of fuel droplets was facilized by the higher temperature at higher loads. The diesel/ethanol blend is observed to have a prolonged ID at low loads and a shortened ID at high loads compared with diesel. This is attributed to the high LHV and low cetane number that come with ethanol, which lowered the cylinder temperature, resulting in a retarded initiation of combustion [11]. However, the cooling effect of ethanol is chipped under higher temperature at higher loads, while the droplet size reduction and oxygen content associated with ethanol significantly shortened the physical and chemical delay period

[47, 54], resulting in a decrement in ID at high loads. As shown, the diesel/ethanol nanofluid presents a shortened ID relative to the diesel/ethanol blend under most conditions. The high thermal conductivity and surface-to-volume ratio of CNPs are responsible for this, as these properties enhance the evaporation rate of fuel droplets and heat transfer between fuel droplets and nanoparticles [49, 55], especially under a high dosage of nanoparticles. The greatest improvement in ID is obtained at 10% load, as CNPs addition could improve the evaporation of fuel droplets by absorbing heat from radiation, therefore lowering the temperature required for auto-ignition [35]. Among all CNPs, as calculated, MWCNT addition has the most pronounced effect on shortening ID, with a reduction by 3.12%, followed by GO and MGO. It can be attributed to its highest improvement for cetane number (see **Table 2**) and the largest surface area (see **Table 1**) with defect bits attached [37], which had a relatively pronounced effect on accelerating the chemical delay period. In comparison with MGO, GO possesses higher thermal diffusivity due to its smaller size (see **Table 1**), thus facilitating the heat transfer and ignition process [56]. Moreover, although GO and MGO show less advantageous in shortening the ID towards MWCNT, they are reported to have a good performance advancing the combustion through special exothermic reactions, which easily occurred under low temperatures, according to the work conducted by Ooi et al. [57].

The combustion duration (CD) for all fuels with a wide range of loading conditions is demonstrated in **Fig.4 (b)**. The combustion duration is usually considered as the crank angle at which the burned mass fraction ranges from 10% to 90%. In the figure, it shows an upward trend of CD with the increasing load, which is due to more time needed to burn more injected fuel. Meanwhile, a shorter CD of the diesel/ethanol blend with respect to diesel is observed. It is because the combustion is accelerated due to the well-distributed air-fuel mixing, which could be attributed to the low viscosity,

boiling point and density of ethanol [48, 58]. Furthermore, the oxygen content of ethanol could alleviate the hypoxia phenomenon during the diffusive combustion [59], especially for high loads, where a larger proportion of diffusion combustion occurs. As in **Fig.4 (b)**, with CNPs added to the diesel/ethanol blend, the CD is reduced generally. The main reason for this is that the high thermal conductivity of CNPs improved the heat transfer rate [22, 55], meanwhile, the high catalytic activity accelerated the combustion reactions [60]. Towards increased load and the nanoparticle dosage, CD shows a decrement trend broadly, indicating that the catalytic effect was enhanced as more catalytic sites and reaction heat were provided, respectively. By calculated, GO performs the best in facilitating the combustion process, with CD decreased by 4.59%, followed by MGO and MWCNT. Compared with MGO, GO possesses a smaller size and higher thermal conductivity, which means a better enhancement for fuel oxidation and heat transfer [21, 61]. The shorter CD for fuels with MGO over MWCNT is mainly because of the inbuilt oxygen of MGO, which promotes the combustion process [22].

Compared with D100, the joint effect of ethanol and CNPs optimizes the combustion process, with the ID and CD decreased by 2.63%, 2.64% at low loads and 2.74%, 6.86% at high loads, respectively. However, this seems unremarkable in comparison to that of the metal-based nanoparticles. According to previous studies, the decrements of 2.9%, 11% and 26% in ID were found after adding alumina [11], titanium dioxide [62] and copper oxide [63], respectively, while the CD reductions of 9.2% [11], 7.7% [64] were achieved by the inclusions of cerium oxide and alumina, respectively. In contrast, the inferior performance towards the combustion process improvement for CNPs is probably attributed to the relatively smaller thermal conductivity and faster degradation rate of carbon-based materials [21, 42]. Nevertheless, it is the rapid decomposition of carbon-based materials during

combustion that results in few residuals of CNPs in the cylinder, therefore compared with metal-based nanoparticles, the long-term operation with CNPs may have less impact on the engine construction.

3.2. *Brake specific fuel consumption and Brake thermal efficiency*

Brake specific fuel consumption (BSFC) is the amount of fuel consumed per kilowatt hour, while the brake thermal efficiency (BTE) defined as the ratio of the power output to the heat equivalent of the burned fuel, which represents the capability to utilize fuel energy. The variations of BSFC and BTE for each tested fuel under various loads are depicted in **Fig.5 (a) and (b)**, respectively.

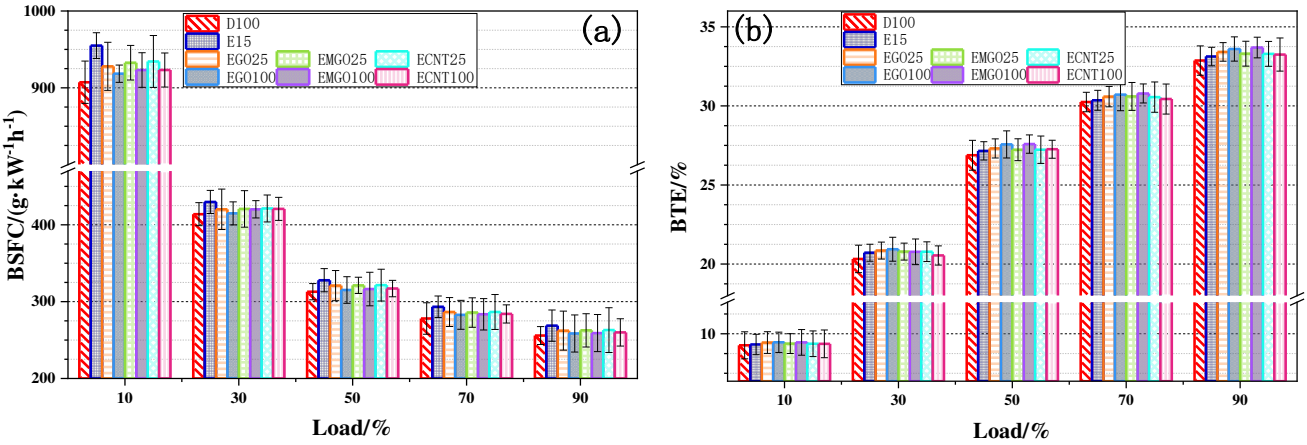

Fig. 5. The diagrams of (a) BSFC and (b) BTE under different loads for all tested fuels.

As in the figure, an increasing trend in BSFC and a decreasing trend in BTE with the growth of load could be observed. This is because the higher temperature of higher loads could promote more complete combustion [65], thus the combustion efficiency got elevated and less fuel is consumed. Compared with diesel, the diesel/ethanol blend exhibits a higher BSFC, as the inclusion of ethanol lowered the calorific value, causing more amount of fuel required to reach the same load [8], especially at high loads, with a maximum increase of 5.48%. However, the blending of ethanol into diesel is observed to present an increment in BTE. It is related to the low density, viscosity and oxygenated nature of ethanol, which improved the combustion characteristics and energy content for fuel [66, 67]. Moreover, the low cetane number associated with ethanol expands the proportion of premixed

combustion, where a better combustion efficiency is reached [68].

In **Fig.5 (a) and (b)**, the diesel/ethanol nanofluids depicts lower BSFC and higher BTE compared with the diesel/ethanol blend. The main reason should be attributed to the violent and rapid droplet breakup associated with the presence of CNPs and ethanol, known as 'micro-explosion', which is favorable for the evaporation and distribution of fuel, in turn enhancing the catalytic activity for CNPs [69, 70]. Therefore, the dispersing of CNPs elevated the density of air-fuel charge and improved the combustion quality [71], especially for low loads, with BSFC decreased by 3.8% and BTE increased by 1.5%. With more CNPs added, both the decrement in BSFC and the increment in BTE are more apparent, indicating a pronounced improvement in the catalytic effect of CNPs. As calculated, GO, MGO and MWCNT decrease the BSFC at ranges of 2.1%-3.8%, 2.0%-3.8%, 1.9%-3.2% and increase the BTE at ranges of 0.6%-1.5%, 0.3%-1.7%, 0.3%-0.8%, respectively. Obviously, the improvements for GO and MGO are comparable, whereas that for MWCNT is the minimum. It is because the oxygenated functional groups within MGO and GO, which were released during combustion, resulted in an elevation in fuel energy content [70]. Compared to D100, the joint effect of CNPs and ethanol has caused slightly higher BSFC but significantly increased BTE. Moreover, the more CNPs added, the more pronounced it presented. When adding ethanol and GO in 100ppm, the optimum improvement in BTE is achieved, ranging in 1.54%-3.02%, only with a little compensation in BSFC, ranging in 0.26%-1.72%. This indicates that under the combined effect of ethanol and CNPs, the engine possesses the better capability to utilize the energy in the fuel, in other words, a better fuel economic performance.

3.3. *Emission characteristics*

3.3.1. Carbon monoxides

The emission of carbon monoxide is aroused from the nonuniform air-fuel mixing, the incomplete combustion and inadequate oxidation [72]. The brake specific emission levels of carbon monoxide (BSCO) emissions for all tested fuels at different loading conditions are shown in **Fig.6.**

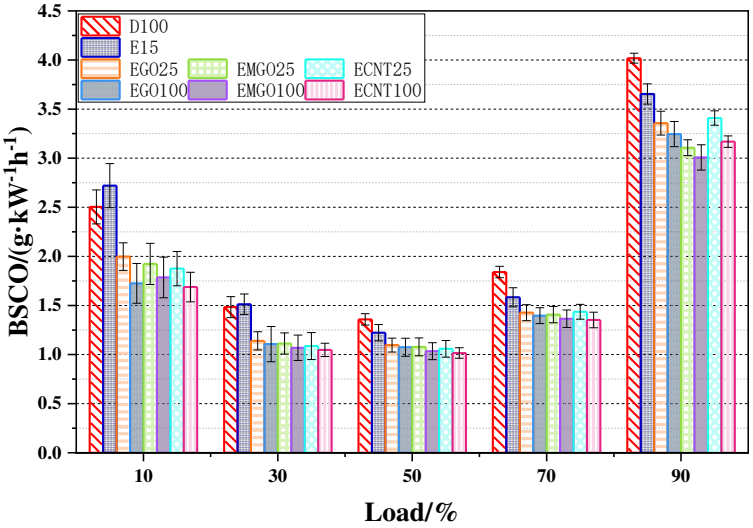

Fig. 6. Measurements of brake specific carbon monoxide emissions under different loads for all tested fuels

In the figure, it is observed a downward trend followed by an upward trend as the load increases, where the minimum BSCO is reached at 50% load. The decrease in BSCO at 10%-50% load is owing to the elevated temperature under increased load, resulting in the complete combustion, while the increase at 50%-90% load is due to the significantly lowered air-fuel ratio with increased load, which hindered the oxidation for fuel. From the graph, it can be observed that compared with diesel, the diesel/ethanol blend has a higher BSCO at low loads but lower BSCO at high loads. The main reason for the increment in BSCO at low loads is that the cooling effect caused by ethanol resulted in a decline in cylinder temperature, giving birth to more incomplete combustion. With the load increased, the cooling effect was suppressed due to the ascended temperature, whereas the oxygen content in ethanol significantly improved the oxidation in rich zones of combustion. However, this result is in contrast to the finding of Rakopoulos et al. [68], who concluded that the incorporation of ethanol could minimize carbon monoxide emissions at low loads. In fact, in their study, the volumetric substitution of ethanol

(5%) was far less than that of this article, affecting the LHV of the fuel to such a minor degree that no cooling effect could be observed, which possibly offered a reason for the discrepancy in the result. The results of this paper are generally concordant with those in prior studies. Zhu et al. [66] revealed that ethanol addition in biodiesel happened to exhibit the cooling effect under light loads when volume substitution of ethanol reaches 10%. Nevertheless, Fang et al. [73] concluded that the ethanol additive had a minimal elevation on carbon monoxide emissions at the injection time of 7.5 ^{o} CA before TDC, providing a fresh method of alleviating the cooling effect brought by alcohol substitution.

In **Fig.6**, it can be seen that the incorporation of CNPs to the diesel/ethanol blend lowers the BSCO detectably, especially at a high dosage of nanoparticles. This is derived from the presence of CNPs homogenized the mixing of fuel and air by promoting the formation of micro-explosion and secondary atomization, then with well contact with fuel, the catalytic reactions were enhanced, leading to a thorough fuel combustion [21, 69]. Among all CNPs, the MWCNT has the greatest improvement in reducing BSCO, with the maximum decrement of 37.95%, followed by GO and MGO. This is because the highest surface-to-volume ratio of MWCNT significantly promoted the combustion reactions, meanwhile, MWCNT acted as a CO_2 absorbent and inhibited any dissociation reaction of CO_2 [42]. The superior effect of GO compared with MGO on reducing the BSCO is because the higher thermal conductivity of GO permits more heat transmitted to the particular fuel molecules, where the catalytic oxidation was improved [74]. Under the joint effect of ethanol and CNPs, the BSCO presents a significant decrement, particularly at low loads, with a maximum of 32.59% for ECNT100. This is consistent with the results found by Ooi et al. [75], who made a comparative investigation on the influences of graphene oxide, single-wall carbon nanotubes and cerium oxide nanoparticles upon the emission behavior for a diesel engine. They revealed that the best optimization for reducing carbon

monoxide is achieved by single-wall carbon nanotubes under low loads, with a decrement of 23.4%. Furthermore, with specific functional groups, the carbon nanoparticles were reported to cause a larger drop in the formation of carbon monoxide, with a reduction by 37.6% for nitrogen-doped MWCNT and 35% for amino-functionalized MWCNT [55, 76].

3.3.2. Hydrocarbons

Fig.7 shows the brake specific hydrocarbon emissions (BSHC) for various fuels under different loads. The main causes for the formation of hydrocarbons are insufficient to fuel evaporation, over-rich or over-lean air-fuel mixture and fuel spray impingement towards the wall [77].

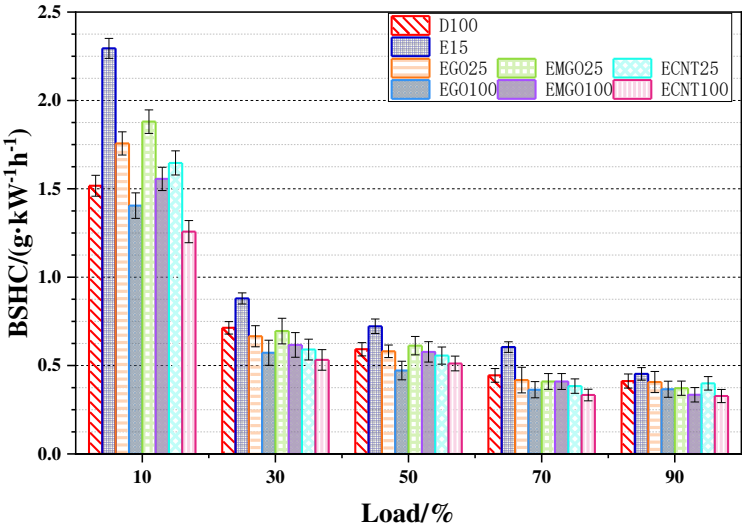

Fig. 7. Measurements of brake specific hydrocarbons emissions under different loads for all tested fuels

In the figure, the BSHC for all tested fuels shows a downward trend with the increasing load, which is mainly caused by the incremental temperature, where complete combustion occurred more easily. As observed, the BSHC for the diesel/ethanol blend is notably higher in comparison with that of diesel. This is due to the leaner air-fuel mixing caused by the oxygen nature of ethanol, which is not favorable for flame propagation [54, 78]. Moreover, the lower viscosity and density of ethanol may lengthen the spray penetration, with more spray impingement towards the cylinder wall. These could be the reasons why the inclusion of ethanol promotes the formation of hydrocarbons. At 10% load, the

maximum increment of 51.24% is obtained, which could be attributed to the high LHV of ethanol, which significantly deteriorates the fuel evaporation efficiency under the low cylinder temperature at low loads. With the load rises, the elevated temperature suppressed the cooling effect, alleviating the increment on hydrocarbon emissions.

In **Fig.7**, the effect of adding CNPs to the diesel/ethanol blend decreases the BSHC, particularly under low loads, with a reduction by 45.18%. It is the high thermal conductivity and pronounced catalytic effect of CNPs that improved the fuel evaporation quality [55, 79] and promoted the oxidation of hydrocarbons [80]. Furthermore, these properties of CNPs shortened the combustion process (see **Fig.4**), lessening the generation time for hydrocarbons [21, 81]. The reduction is observed to get significant with more CNPs added, indicating that a high catalytic activity is presented under a high nanoparticle concentration. By contrast, the MWCNT has the greatest reduction in BSHC, with a maximum decrease by 45.18% for ECNT100. It is associated with the highest specific area and thermal conductivity of MWCNT, which significantly optimizes the evaporation and oxidation of fuel [69]. Compared with D100, the BSHC for fuel is decreased under the joint effect of CNPs and ethanol, especially in a high dosage of nanoparticles. The optimum reduction of 25.42% in BSHC was attained with the addition of ethanol and GO at 100ppm.

3.3.3. Nitrogen Oxides

Fig.8 shows the brake specific nitrogen oxides ($BSNO_X$) emission for various fuels with different loading conditions. Generated from the chemical reactions between nitrogen and oxygen under a high temperature environment, the nitrogen oxide emission is mainly affected by the combustion temperature, local oxygen and the residence time under high temperatures.

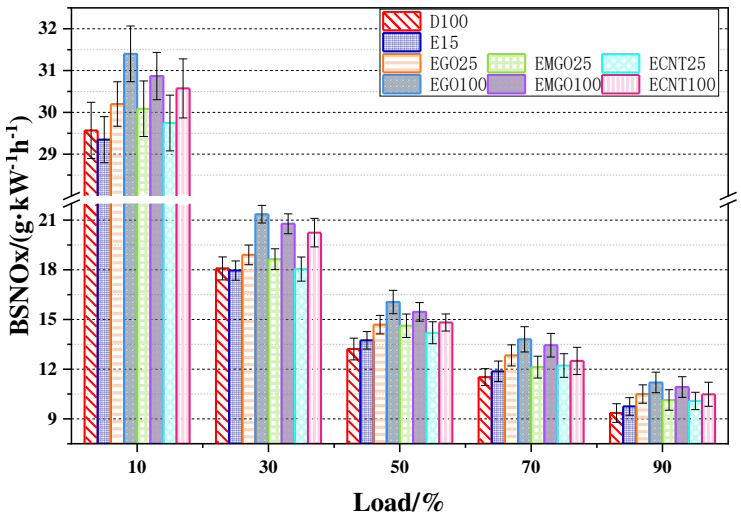

Fig. 8. Measurements of brake specific nitrogen oxides emissions under different loads for all tested fuels

As shown in the figure, as the cylinder temperature and combustion duration are elevated, the emissions of nitrogen oxide do increase with increasing load. However, the output power presents a greater increase, consequently resulting in a decreasing trend in $BSNO_X$, as shown in the figure. With the load increases, the blending of ethanol into diesel is observed to have a notable decline at low loads and an increase at high loads. The decline at low loads is aroused from the cooling effect due to the high LHV and low cetane number associated with ethanol, which reduced the temperature significantly under low loads, leading to a lower $BSNO_X$. However, the cooling effect is chipped under the higher temperature of higher load, whereas the bounded oxygen of ethanol promoted oxidation of the fuel significantly at high loads, with more nitrogen oxides formed.

As shown in **Fig.8**, the CNPs addition increases the $BSNO_X$ regardless of the loading conditions, especially for the high concentration. This is because the high thermal conductivity and large specific surface area of CNPs enhanced the complete combustion remarkably, increasing the cylinder pressure and corresponding temperature, thus a significant increment on $BSNO_X$ is obtained at high loads [82, 83]. Specifically, the oxygen functional groups in GO and MGO assisted the oxidation of nitrogen [21], implying higher $BSNO_X$ for GO and MGO relative to MWCNT.

Compared with D100, under the combined effect of ethanol and CNPs, $BSNO_X$ is elevated by 5.22%-21.46%. In detail, the EGO25/EGO100, EMGO25/EMGO100, ECNT25/ECNT100 present increments in the ranges of 2.14%-12.23%/6.19%-21.46%, 1.75%-10.63%/4.4%-16.95%, 0.6%-7.83%/3.4%-12.11% on $BSNO_X$, respectively. Obviously, the highest increment in nitrogen oxides emission is obtained for the fuel with GO added in 100ppm. However, the increments are not apparent when compared with the results from other studies. As previous research reported, the addition of alumina, ceria and titanium dioxide into the fuel brought about further higher increase in emissions of nitrogen oxides, which is up to 40% [44], 27.8% [84], 31.87% [85]. By contrast, increase in $BSNO_X$ caused by the joint effect of ethanol and CNPs is more acceptable.

3.3.4. Smoke opacity

The smoke opacity reflected the emission of soot, which mainly comes from the partial reactions between carbon atoms within the fuel and the incomplete combustion of hydrocarbons. **Fig.9** demonstrates the variation of smoke opacity across various fuels at different loading conditions.

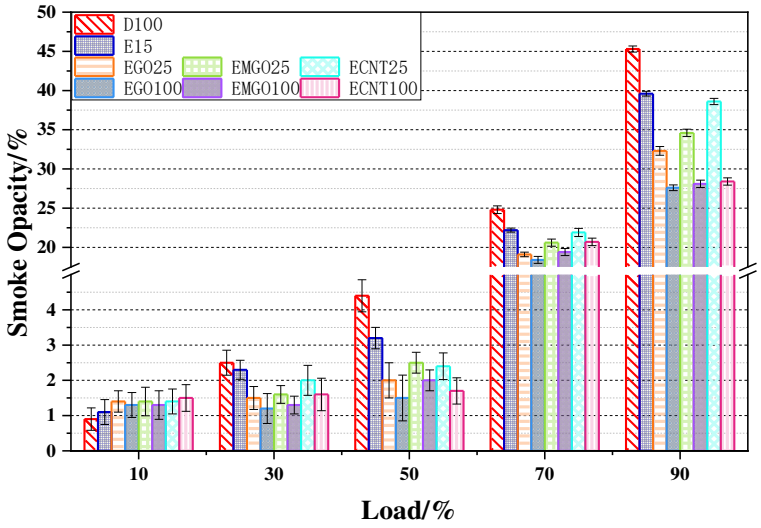

Fig. 9. Measurements of smoke opacity under different loads for all tested fuels

In this figure, it can be observed that the smoke opacity has an increasing tendency with the rise of load. This is because with more fuel injected at a higher load, the air-fuel mixture got richer,

followed with more incomplete combustion, and then more soot was generated. Compared with diesel, the smoke opacity of the diesel/ethanol blend was higher under low loads yet lower under high loads. This is mainly driven by a reduction in cylinder temperature as a result of the high LHV associated with ethanol, which significantly resulted in more incomplete combustion under the low temperature at low loads. However, it is suppressed at higher loading conditions for higher temperatures, whereas the oxygenated nature of ethanol promotes the oxidation in rich zones of combustion and the low density, viscosity contribute to the well distribution of fuel, causing a reduction in the formation of soot nuclei [73, 86]. Furthermore, the radicals of HO_2 and OH released from the combustion of ethanol would consume the polycyclic aromatic hydrocarbon, suppressing the nucleation of smoke particles [87].

In **Fig.9**, after adding CNPs into the diesel/ethanol blend, the smoke opacity for fuels is increased at low loads and decreased at high loads. The increment at low loads is because, in the case of the short combustion duration of low loads, CNPs could not burn out in time, thus acting as soot nucleus and promoting the generation of smoke particles [56]. Under high loads, with sufficient residence time to burn, this phenomenon was diminished naturally, while the atomization and heat propagation of fuel were significantly improved by CNPs [21, 37], inhibiting the formation of smoke particles, especially towards more CNPs added. Particularly, the structural oxygen of GO and MGO released enough oxygen for oxidation [22, 88], leading to the reduction in soot emissions, which may indicate the larger soot emission reduction for GO and MGO compared with that for MWCNT. In detail, GO and MGO contribute to the soot emission decrease in the ranges of 13.96%-47.82% and 7.2%-43.48%, and it is obvious that GO possesses better capability in reducing soot emissions relative to MGO. This could be attributed to the higher thermal conductivity and smaller size of GO, which is conducive to fuel

oxidation [51]. By comparison with diesel, impacted by the joint effect of ethanol and CNPs, the smoke opacity is reduced in ranges of 22.98%-65.91%, 16.54%-54.54%, 11.69%-61.36% for EGO100, EMGO100, EMWCNT100, respectively. It indicates that the joint effect of ethanol and CNPs has the collective capability to inhibit the soot emission of the diesel engine.

3.4. *Discussion on the present results*

In order to evaluate various joint effects of ethanol and CNPs with different types (GO, MGO, MWCNT) and dosages (25ppm, 100ppm), Δ_x, a normalized parameter, is defined by **Eq. (1)** and listed in **Table 5**, which measured the maximum relative variation on the corresponding characteristic parameter at all the loading conditions raised by a specific combination of ethanol and CNPs relative to diesel fuel.

$$\Delta_x = \max_{1\le j\le 5}\left(\left|\frac{x_{EZi,a_j}-x_{D100,a_j}}{x_{D100,a_j}}\right|\right), (\mathrm{i}=25,100,\mathrm{a_j}=10\%,\ 30\%,\ 50\%,\ 70\%,\ 90\%) \quad (1)$$

In the above equation, Z means the type of the added CNPs, including GO, MGO and CNT, while x_{EZi,a_j} and x_{D100,a_j} represent tested parameters for EZi and $D100$ at a_j load, respectively. "x" denotes the characteristic parameters, including peak CGP, peak HRR, ID, CD, BSFC, BTE, as well as emissions in CO, HC, NOx and smoke.

Table 5. Summary of the maximum variations raised by the combination of ethanol and CNPs.

	Ethanol+GO[a]		Ethanol+MGO		Ethanol+MWCNT	
	25ppm[b]	100ppm	25ppm	100ppm	25ppm	100ppm
$\Delta_{peak\ CGP}$	4.13%$_{(90\%)}$[c] ↑[d]	6.29%$_{(90\%)}$ ↑	3.82%$_{(90\%)}$ ↑	6.12%$_{(90\%)}$ ↑	3.71%$_{(90\%)}$ ↑	5.77%$_{(90\%)}$ ↑
$\Delta_{peak\ HRR}$	12.30%$_{(90\%)}$↑	16.45%$_{(90\%)}$↑	12.65%$_{(90\%)}$↑	16.33%$_{(90\%)}$↑	11.55%$_{(90\%)}$↑	12.57%$_{(90\%)}$↑
Δ_{ID}	1.95%$_{(70\%)}$ ↓	3.47%$_{(50\%)}$ ↓	1.77%$_{(70\%)}$ ↓	2.74%$_{(70\%)}$ ↓	2.63%$_{(30\%)}$ ↓	3.51%$_{(50\%)}$ ↓
Δ_{CD}	5.51%$_{(90\%)}$ ↓	6.33%$_{(90\%)}$ ↓	4.63%$_{(70\%)}$ ↓	6.86%$_{(90\%)}$ ↓	4.62%$_{(70\%)}$ ↓	5.85%$_{(90\%)}$ ↓
Δ_{BSFC}	3.03%$_{(70\%)}$ ↑	1.72%$_{(70\%)}$ ↑	2.81%$_{(10\%)}$ ↑	1.96%$_{(70\%)}$ ↑	3.03%$_{(70\%)}$ ↑	2.13%$_{(70\%)}$ ↑
Δ_{BTE}	2.61%$_{(30\%)}$ ↑	3.02%$_{(30\%)}$ ↑	2.28%$_{(30\%)}$ ↑	2.63%$_{(50\%)}$ ↑	2.25%$_{(30\%)}$ ↑	1.42%$_{(50\%)}$ ↑
Δ_{CO}	23.16%$_{(30\%)}$↓	31.09%$_{(10\%)}$↓	24.99%$_{(30\%)}$↓	28.69%$_{(10\%)}$↓	26.74%$_{(30\%)}$↓	32.59%$_{(10\%)}$↓
Δ_{HC}	6.68%$_{(30\%)}$ ↓	20.36%$_{(50\%)}$↓	9.79%$_{(90\%)}$ ↓	18.82%$_{(90\%)}$↓	17.22%$_{(30\%)}$↓	25.42%$_{(30\%)}$↓
Δ_{NOx}	12.29%$_{(90\%)}$↑	21.46%$_{(50\%)}$↑	10.63%$_{(50\%)}$↑	16.95%$_{(50\%)}$↑	7.83%$_{(90\%)}$ ↑	12.11%$_{(50\%)}$↑
Δ_{smoke}	54.55%$_{(50\%)}$↓	65.91%$_{(50\%)}$↓	43.18%$_{(50\%)}$↓	54.55%$_{(50\%)}$↓	45.45%$_{(50\%)}$↓	61.36%$_{(50\%)}$↓

Note: [a] Ethanol+GO means the combined additive of ethanol and GO.

[b] 25ppm represents the incorporation of CNPs at a dose of 25 ppm.

[c] $4.13\%_{(90\%)}$ is denoted as the maximum variation of 4.13% occurred at 90% load.

[d] "↑" means that the characteristic parameter is elevated by the combination of ethanol and CNPs, while "↓"notes that the combination of ethanol and CNPs decreases the characteristic parameter.

As shown in the **Table 5**, driven by the combined impact of ethanol and CNPs, some characteristics of the engine are considerably optimized, involving elevations in Peak CGP, Peak HRR and BTE, as well as drops in ID, CD and emission in CO, HC and smoke, whereas other characteristics of the engine are deteriorated, with elevated BSFC and NOx emission. Within all combinations on CNPs and ethanol, the combination of ethanol and GO (100ppm) delivers the highest improvements on Peak CGP, Peak HRR, CD, BTE and smoke emission, while the combination of ethanol and MWCNT (100ppm) contributes to the optimal enhancements on ID and emissions in CO and HC. In addition, the mildest increments on BSFC and NOx emission are accomplished by the combination of ethanol and GO (100ppm) and the combination of ethanol and MWCNT (25ppm), respectively. Without doubts, benefited from the oxygenated nature, the combination of ethanol and GO (100ppm) greatly supplements the oxygen content of the fuel, thus dramatically boosting the combustion process, fuel utilization and smoke emission minimization, especially at medium or high loads. However, with the activated oxidation reaction, the combination of ethanol and GO (100ppm) equally introduced a maximum growth on NOx emission. While thanks to the minimal oxygen content of MWCNT, the combination of ethanol and MWCNT (25ppm) minimized NOx generation. Moreover, due to the maximum specific surface area possessed by MWCNT, the combination of ethanol and MWCNT (100ppm) offers a pronounced abatement effect in CO, HC and smoke emissions, especially at low loads. Besides, considering that the combination of ethanol and MWCNT (100ppm) equally resulted in the shortest ID, it can be inferred that certain reactions within ignition delay may be relevant to the abatement mechanisms, which is particularly enhanced by the MWCNT. Therefore, with respect to

engine emissions control, the employment of the combination of ethanol and MWCNT (100ppm) as a fuel additive under low loads represents a favorable choice, yet in view of the improvements in combustion and performance characteristics of the engine, the combined fuel additive involved ethanol and GO (100ppm) ought to be preferred for the utilization at medium or high loads.

4. Conclusion

This paper focuses on the impacts of three strings of renewable carbon nanoparticles (graphene oxides, GO; the multi-layered graphene oxides, MGO; the multi-walled carbon nanotubes, MWCNT) towards combustion, performance and emission behavior in the diesel engine under various loading conditions at 1200rpm. Based on the findings, the main conclusions are drawn:

Inclusion of CNPs into the diesel/ethanol blend significantly benefits the combustion progress, contributing to an increase in peak cylinder gas pressure (peak CGP) and peak heat release rate (peak HRR), as well as a reduction in ignition delay (ID) and combustion duration (CD). The GO aroused the most significant improvement in combustion process, followed by MGO and MWCNT.

The incorporation of CNPs in the diesel/ethanol blend could significantly improve fuel utilization with a reduced BSFC and a correspondingly increased BTE. Naturally, in contrast to pure diesel fuel, co-effects of CNPs and ethanol present an elevated BTE with only a small compensation in BSFC, especially for GO, with an increase in the ranges of 2.1%-3.8% for BTE and 0.5%-1.5% for BSFC.

The incorporation of CNPs upon the diesel/ethanol blend decreased the emissions in carbon monoxide (CO), hydrocarbon (HC) and smoke opacity, but also increased nitrogen oxides (NOx) emissions. MWCNT has the most noticeable decreasing effect on the emissions of CO and HC, while the maximum decremental effect on smoke opacity is observed for GO.

Different combinations of ethanol and CNPs result in differing improvements in the characteristics

of the engine. The application of the combination of ethanol and GO (100ppm) at medium and high loads resulted in favorable improvements in the combustion process and fuel economy, whereas the combination of ethanol and MWCNT (100ppm) caused the optimal enhancements in emission control when operated at low loads.

Overall, the investigation revealed that the combination of ethanol and CNPs improved the combustion process and reduced CO, HC and soot emissions, yet NOx emissions slightly increased. Considering the increase in NOx emissions, more specifically targeted studies should be developed to obtain an integrated and effective emission control e.g. using other nanoparticles, employing post-treatment devices, operating with exhaust gas recirculation, etc. Further, the greatest improvement to the combustion process is obtained with GO involved, whereas the overall emission abatement effect is the strongest with MWCNT incorporated, so it seems that there exists a trade-off between combustion improvement and emission reduction. From this perspective, the authors suggest investigating the mixing of these two nanoparticles at different proportions to promote high-efficiency combustion with minimal emissions.

Acknowledgments

This research is supported by Anhui Provincial Natural Science Foundation (2308085ME175), the Fundamental Research Funds for the Central Universities (300102384501, JZ2024HGTG0302), Yangtze River Delta Science and Technology Innovation Community Collaborative Research Program (SQ2024CSJGG0024) and Hefei Municipal Natural Science Foundation and the Fundamental (JZ2024HKZR0707).

References

[1] Agarwal A K. Biofuels (alcohols and biodiesel) applications as fuels for internal combustion engines [J]. Progress in Energy and Combustion Science, 2007, 33(3): 233-271.

[2] E J, Minhhieu P, Zhao D, et al. Effect of different technologies on combustion and emissions of the diesel engine fueled with biodiesel: A review [J]. Renewable & Sustainable Energy Reviews, 2017, 80: 620-647.
[3] Chen H, Su X, Li J, et al. Effects of gasoline and polyoxymethylene dimethyl ethers blending in diesel on the combustion and emission of a common rail diesel engine [J]. Energy, 2019, 171: 981-999.
[4] Chen H, Xie B, Ma J Q, et al. NOx emission of biodiesel compared to diesel: Higher or lower? [J]. Applied Thermal Engineering, 2018, 137: 584-593.
[5] Hoseini S S, Najafi G, Ghobadian B, et al. The effect of combustion management on diesel engine emissions fueled with biodiesel-diesel blends [J]. Renewable & Sustainable Energy Reviews, 2017, 73: 307-331.
[6] Mishra P C, Gupta A, Kumar A, et al. Methanol and petrol blended alternate fuel for future sustainable engine: A performance and emission analysis [J]. Measurement, 2020, 155: 107519.
[7] Duraisamy G, Rangasamy M, Govindan N. A comparative study on methanol/diesel and methanol/PODE dual fuel RCCI combustion in an automotive diesel engine [J]. Renewable Energy, 2020, 145: 542-556.
[8] Rakopoulos D C, Rakopoulos C D, Papagiannakis R G, et al. Combustion heat release analysis of ethanol or n-butanol diesel fuel blends in heavy-duty DI diesel engine [J]. Fuel, 2011, 90(5): 1855-1867.
[9] Huang Y-H, Wu J-H. Analysis of biodiesel promotion in Taiwan [J]. Renewable & Sustainable Energy Reviews, 2008, 12(4): 1176-1186.
[10] Yucesu H S, Topgul T, Cinar C, et al. Effect of ethanol-gasoline blends on engine performance and exhaust emissions in different compression ratios [J]. Applied Thermal Engineering, 2006, 26(17-18): 2272-2278.
[11] Chen Q, Wang C, Shao K, et al. Analyzing the combustion and emissions of a DI diesel engine powered by primary alcohol (methanol, ethanol, n-butanol)/diesel blend with aluminum nano-additives [J]. Fuel, 2022, 328.
[12] Yin X, Ren X, Luan J, et al. Effect of Methanol Energy Substitution Ratio on Performance of Methanol/Diesel Dual-Direct Injection Engine [J]. Hsi-An Chiao Tung Ta Hsueh/Journal of Xi'an Jiaotong University, 2023, 57(9): 71-78.
[13] Feng S, Zhang S, Zhang H, et al. Effect of nozzle geometry on combustion of a diesel-methanol dual-fuel direct injection engine [J]. Fuel, 2024, 357.
[14] Jamrozik A, Tutak W, Pyrc M, et al. Study on co-combustion of diesel fuel with oxygenated alcohols in a compression ignition dual-fuel engine [J]. Fuel, 2018, 221: 329-345.
[15] Wai P, Kanokkhanarat P, Oh B-S, et al. Experimental investigation of the influence of ethanol and biodiesel on common rail direct injection diesel Engine's combustion and emission characteristics [J]. Case Studies in Thermal Engineering, 2022, 39: 102430.
[16] Suresh Kumar P, Prasanthi Kumari N, Sharma A K. Cut-off percentage of ethanol in diesel-biodiesel based fuel blends and analysis of emissions in four stroke-compression ignition engines [J]. Nature Environment and Pollution Technology, 2021, 20(2): 619-624.
[17] Anandkumar G, Sasikala V, Rao B P C, et al. Effect of CNG Induction on the Performance and Emission Characteristics of a DI Diesel Engine Fuelled with Biodiesel Ethanol Blends [J]. International Journal of Vehicle Structures and Systems, 2023, 15(5): 680-683.
[18] Chen H, Su X, He J, et al. Investigation on combustion and emission characteristics of a common rail diesel engine fueled with diesel/n-pentanol/methanol blends [J]. Energy, 2019, 167: 297-311.
[19] Simhadri K, Rao P S, Paswan M. Improving the combustion and emission performance of a diesel engine with TiO2 nanoparticle blended Mahua biodiesel at different injection pressures [J]. International Journal of Thermofluids, 2024, 21: 100563.
[20] El-Seesy A I, Waly M S, He Z, et al. Enhancement of the combustion and stability aspects of diesel-methanol-hydrous methanol blends utilizing n-octanol, diethyl ether, and nanoparticle additives [J]. Journal of Cleaner Production, 2022, 371: 133673.
[21] Chacko N, Jeyaseelan T. Comparative evaluation of graphene oxide and graphene nanoplatelets as fuel additives

on the combustion and emission characteristics of a diesel engine fuelled with diesel and biodiesel blend [J]. Fuel Processing Technology, 2020, 204.

[22] Soudagar M E M, Nik-Ghazali N-N, Kalam M A, et al. The effects of graphene oxide nanoparticle additive stably dispersed in dairy scum oil biodiesel-diesel fuel blend on CI engine: performance, emission and combustion characteristics [J]. Fuel, 2019, 257.

[23] Rajesh K, Bibin C, Soundararajan G, et al. Investigating the impact of alumina nanoparticles in coconut oil distillate biodiesel to lessen emissions in direct injection diesel engine [J]. Scientific Reports, 2024, 14(1): 13228.

[24] Xu M, Niu Z, Shi Z, et al. High-Resolution Characterization of Coal Combustion-Derived Metal-Containing Nanoparticles and Their Health-Related Implications [J]. Environmental Science & Technology Letters, 2024.

[25] Prabu S, Vinu M, Chiang K-Y. Temperature-dependent highly active LaCaMgAl2O4 catalyst effect on carbon nanomaterial and hydrogen generation from polymethyl methacrylate plastic [J]. Chemosphere, 2024, 366: 143540.

[26] He Z, Lin H, Sui J, et al. Seafood waste derived carbon nanomaterials for removal and detection of food safety hazards [J]. Science of The Total Environment, 2024, 929: 172332.

[27] Soudagar M E M, Nik-Ghazali N-N, Kalam M A, et al. The effect of nano-additives in diesel-biodiesel fuel blends: A comprehensive review on stability, engine performance and emission characteristics [J]. Energy Conversion and Management, 2018, 178: 146-177.

[28] Chebattina K R, Srinivas V, Rao N M. Influence of Size and Weight Fraction of Multi-Walled Carbon Nanotubes Dispersed in Gear Oils for Improvement of Tribological Properties [J]. Journal of the Chinese Society of Mechanical Engineers, 2021, 42(1): 63-71.

[29] Lipomi D J, Vosgueritchian M, Tee B C K, et al. Skin-like pressure and strain sensors based on transparent elastic films of carbon nanotubes [J]. Nature Nanotechnology, 2011, 6(12): 788-792.

[30] Won S, Jang J-W, Choi H-J, et al. A graphene meta-interface for enhancing the stretchability of brittle oxide layers [J]. Nanoscale, 2016, 8(9): 4961-4968.

[31] Gui P, Long W, Cai X, et al. Influence analysis of lubrication and friction reduction of graphene oxide lubricant at SiC interface [J]. Colloids and Surfaces A: Physicochemical and Engineering Aspects, 2024, 691: 133897.

[32] Kaleli E H, Demirtaş S. Experimental investigation of the effect of tribological performance of reduced graphene oxide additive added into engine oil on gasoline engine wear [J]. Lubrication Science, 2023, 35(2): 118-143.

[33] Ma S, Guo Q, Wei J, et al. Analyzing the effect of carbon nanoparticles on the combustion performance and emissions of a DI diesel engine fueled with the diesel-methanol blend [J]. Energy, 2024, 300.

[34] Selvan V a M, Anand R B, Udayakumar M. Effect of Cerium Oxide Nanoparticles and Carbon Nanotubes as fuel-borne additives in Diesterol blends on the performance, combustion and emission characteristics of a variable compression ratio engine [J]. Fuel, 2014, 130: 160-167.

[35] Ooi J B, Ismail H M, Swamy V, et al. Graphite Oxide Nanoparticle as a Diesel Fuel Additive for Cleaner Emissions and Lower Fuel Consumption [J]. Energy & Fuels, 2016, 30(2): 1341-1353.

[36] Najafi G. Diesel engine combustion characteristics using nano-particles in biodiesel-diesel blends [J]. Fuel, 2018, 212: 668-678.

[37] Mei D, Zuo L, Adu-Mensah D, et al. Combustion characteristics and emissions of a common rail diesel engine using nanoparticle-diesel blends with carbon nanotube and molybdenum trioxide [J]. Applied Thermal Engineering, 2019, 162.

[38] Manigandan S, Sarweswaran R, Booma Devi P, et al. Comparative study of nanoadditives TiO2, CNT, Al2O3, CuO and CeO2 on reduction of diesel engine emission operating on hydrogen fuel blends [J]. Fuel, 2020, 262: 116336.

[39] Maleki A, Hamesadeghi U, Daraei H, et al. Amine functionalized multi-walled carbon nanotubes: Single and binary CI crossmark systems for high capacity dye removal [J]. Chemical Engineering Journal, 2017, 313: 826-835.

[40] Tian J, Tan Y, Zhang Z, et al. Effects of hyperbranched polyesters covalent functionalized multi-walled carbon nanotubes on the mechanical and tribological properties of epoxy composites [J]. Materials Research Express, 2020, 7(1).
[41] Arvand M, Palizkar B. Development of a modified electrode with amine-functionalized TiO2/multi-walled carbon nanotubes nanocomposite for electrochemical sensing of the atypical neuroleptic drug olanzapine [J]. Materials Science and Engineering C, 2013, 33(8): 4876-4883.
[42] Waly M S, El-Seesy A I, El-Batsh H M, et al. Combustion and emissions characteristics of a diesel engine fuelled with diesel fuel and different concentrations of amino-functionalized multi-walled carbon nanotube [J]. Atmospheric Pollution Research, 2023, 14(8).
[43] El-Seesy A I, Attia A M A, El-Batsh H M. The effect of Aluminum oxide nanoparticles addition with Jojoba methyl ester-diesel fuel blend on a diesel engine performance, combustion and emission characteristics [J]. Fuel, 2018, 224: 147-166.
[44] Wei J, He C, Fan C, et al. Comparison in the effects of alumina, ceria and silica nanoparticle additives on the combustion and emission characteristics of a modern methanol-diesel dual-fuel CI engine [J]. Energy Conversion and Management, 2021, 238.
[45] Liu J, Yang J, Sun P, et al. Compound combustion and pollutant emissions characteristics of a common-rail engine with ethanol homogeneous charge and polyoxymethylene dimethyl ethers injection [J]. Applied Energy, 2019, 239: 1154-1162.
[46] Lu X C, Yang J G, Zhang W G, et al. Effect of cetane number improver on heat release rate and emissions of high speed diesel engine fueled with ethanol-diesel blend fuel [J]. Fuel, 2004, 83(14-15): 2013-2020.
[47] Venu H, Raju V D, Lingesan S, et al. Influence of Al2O3 nano additives in ternary fuel (diesel-biodiesel-ethanol) blends operated in a single cylinder diesel engine: Performance, combustion and emission characteristics [J]. Energy, 2021, 215.
[48] Qi D H, Chen H, Geng L M, et al. Effect of diethyl ether and ethanol additives on the combustion and emission characteristics of biodiesel-diesel blended fuel engine [J]. Renewable Energy, 2011, 36(4): 1252-1258.
[49] Billa K K, Deb M, Sastry G R K, et al. Experimental investigation on dispersing graphene-oxide in biodiesel/diesel/higher alcohol blends on diesel engine using response surface methodology [J]. Environmental Technology, 2022, 43(20): 3131-3148.
[50] Gad M S, Abulut U, Afzal A, et al. A comprehensive review on the usage of the nano-sized particles along with diesel/biofuel blends and their impacts on engine behaviors [J]. Fuel, 2023, 339.
[51] Hosseinzadeh-Bandbafha H, Khalife E, Tabatabaei M, et al. Effects of aqueous carbon nanoparticles as a novel nanoadditive in water-emulsified diesel/biodiesel blends on performance and emissions parameters of a diesel engine [J]. Energy Conversion and Management, 2019, 196: 1153-1166.
[52] Cheng C, Faurskov Cordtz R, Dyhr Pedersen T, et al. Investigation of combustion characteristics, physical and chemical ignition delay of methanol fuel in a heavy-duty turbo-charged compression ignition engine [J]. Fuel, 2023, 348: 128536.
[53] Venkatesan H, Udhaya Kumar V, Sivamani S, et al. Evaluation of combustion, performance and emission characteristics of a diesel engine fuelled with diesel–jojoba biodiesel–n butanol with multi-walled carbon nanotube as fuel additive [J]. International Journal of Ambient Energy, 2023, 44(1): 1748-1766.
[54] Rakopoulos D C, Rakopoulos C D, Giakoumis E G, et al. Influence of properties of various common bio-fuels on the combustion and emission characteristics of high-speed DI (direct injection) diesel engine: Vegetable oil, bio-diesel, ethanol, n-butanol, diethyl ether [J]. Energy, 2014, 73: 354-366.
[55] El-Seesy A I, Waly M S, El-Batsh H M, et al. Enhancement of the diesel fuel characteristics by using nitrogen-doped multi-walled carbon nanotube additives [J]. Process Safety and Environmental Protection, 2023, 171: 561-

577.
[56] Zhang Z, Lu Y, Wang Y, et al. Comparative study of using multi-wall carbon nanotube and two different sizes of cerium oxide nanopowders as fuel additives under various diesel engine conditions [J]. Fuel, 2019, 256.
[57] Ooi J B, Rajanren J R, Ismail H M, et al. Improving combustion characteristics of diesel and biodiesel droplets by graphite oxide addition for diesel engine applications [J]. International Journal of Energy Research, 2017, 41(14): 2258-2267.
[58] Wei L, Yao C, Wang Q, et al. Combustion and emission characteristics of a turbocharged diesel engine using high premixed ratio of methanol and diesel fuel [J]. Fuel, 2015, 140: 156-163.
[59] Hulwan D B, Joshi S V. Performance, emission and combustion characteristic of a multicylinder DI diesel engine running on diesel-ethanol-biodiesel blends of high ethanol content [J]. Applied Energy, 2011, 88(12): 5042-5055.
[60] Bikkavolu J R, Vadapalli S, Chebattina K R R, et al. Effects of stably dispersed carbon nanotube additives in yellow oleander methyl ester-diesel blend on the performance, combustion, and emission characteristics of a CI engine [J]. Biofuels-Uk, 2023.
[61] Esfahani M R, Languri E M, Nunna M R. Effect of particle size and viscosity on thermal conductivity enhancement of graphene oxide nanofluid [J]. International Communications in Heat and Mass Transfer, 2016, 76: 308-315.
[62] Gad M S, Abdel Aziz M M, Kayed H. Impact of different nano additives on performance, combustion, emissions and exergetic analysis of a diesel engine using waste cooking oil biodiesel [J]. Propulsion and Power Research, 2022, 11(2): 209-223.
[63] Rastogi P M, Sharma A, Kumar N. Effect of CuO nanoparticles concentration on the performance and emission characteristics of the diesel engine running on jojoba (Simmondsia Chinensis) biodiesel [J]. Fuel, 2021, 286: 119358.
[64] Pan S, Wei J, Tao C, et al. Discussion on the combustion, performance and emissions of a dual fuel diesel engine fuelled with methanol-based CeO2 nanofluids [J]. Fuel, 2021, 302.
[65] Zenghui Y, Jing H, Jiangjun W. Study on the influence of alumina nanomethanol fluid on the performance, combustion and emission of DMDF diesel engine [J]. E3S Web of Conferences, 2021, 268: 01004 (01015 pp.)-01004 (01015 pp.).
[66] Zhu L, Cheung C S, Zhang W G, et al. Combustion, performance and emission characteristics of a DI diesel engine fueled with ethanol-biodiesel blends [J]. Fuel, 2011, 90(5): 1743-1750.
[67] Balamurugan T, Nalini R. Experimental investigation on performance, combustion and emission characteristics of four stroke diesel engine using diesel blended with alcohol as fuel [J]. Energy, 2014, 78: 356-363.
[68] Rakopoulos D C, Rakopoulos C D, Kakaras E C, et al. Effects of ethanol-diesel fuel blends on the performance and exhaust emissions of heavy duty DI diesel engine [J]. Energy Conversion and Management, 2008, 49(11): 3155-3162.
[69] Basha J S, Anand R B. An experimental investigation in a diesel engine using carbon nanotubes blended water-diesel emulsion fuel [J]. Proceedings of the Institution of Mechanical Engineers Part a-Journal of Power and Energy, 2011, 225(A3): 279-288.
[70] Khan H, Manzoore Elahi M S, Rajagopal H K, et al. Effect of Nano-Graphene Oxide and n-Butanol Fuel Additives Blended with Diesel—Nigella sativa Biodiesel Fuel Emulsion on Diesel Engine Characteristics [J]. Symmetry, 2020, 12(6): 961.
[71] Gan Y, Qiao L. Evaporation characteristics of fuel droplets with the addition of nanoparticles under natural and forced convections [J]. International Journal of Heat and Mass Transfer, 2011, 54(23-24): 4913-4922.
[72] Muralidharan K, Vasudevan D. Performance, emission and combustion characteristics of a variable compression ratio engine using methyl esters of waste cooking oil and diesel blends [J]. Applied Energy, 2011, 88(11): 3959-3968.

[73] Fang Q, Fang J, Zhuang J, et al. Effects of ethanol-diesel-biodiesel blends on combustion and emissions in premixed low temperature combustion [J]. Applied Thermal Engineering, 2013, 54(2): 541-548.
[74] El-Seesy A I, Nour M, Hassan H, et al. Diesel-oxygenated fuels ternary blends with nano additives in compression ignition engine: A step towards cleaner combustion and green environment [J]. Case Studies in Thermal Engineering, 2021, 25: 100911.
[75] Ooi J B, Ismail H M, Tan B T, et al. Effects of graphite oxide and single-walled carbon nanotubes as diesel additives on the performance, combustion, and emission characteristics of a light-duty diesel engine [J]. Energy, 2018, 161: 70-80.
[76] El-Seesy A I, Waly M S, El-Batsh H M, et al. Enhancement of the waste cooking oil biodiesel usability in the diesel engine by using n-decanol, nitrogen-doped, and amino-functionalized multi-walled carbon nanotube [J]. Energy Conversion and Management, 2023, 277: 116646.
[77] Venu H, Madhavan V. Influence of diethyl ether (DEE) addition in ethanol-biodiesel-diesel (EBD) and methanol-biodiesel-diesel (MBD) blends in a diesel engine [J]. Fuel, 2017, 189: 377-390.
[78] Azad A K, Halder P, Wu Q, et al. Experimental investigation of ternary biodiesel blends combustion in a diesel engine to reduce emissions [J]. Energy Conversion and Management: X, 2023, 20: 100499.
[79] El-Seesy A I, Hassan H, Ookawar S. Performance, combustion, and emission characteristics of a diesel engine fueled with Jatropha methyl ester and graphene oxide additives [J]. Energy Conversion and Management, 2018, 166: 674-686.
[80] Mohanrajhu N, Sekar S, Jayabal R, et al. Impact of Aluminum Nitrate and Graphene Oxide Nanoplate on Performance and Emission Characteristics of a CRDI Diesel Engine Powered by Industrial Leather Waste Fat Biodiesel [J]. International Journal of Automotive Technology, 2024.
[81] El-Seesy A I, Abdel-Rahman A K, Bady M, et al. Performance, combustion, and emission characteristics of a diesel engine fueled by biodiesel-diesel mixtures with multi-walled carbon nanotubes additives [J]. Energy Conversion and Management, 2017, 135: 373-393.
[82] Ooi J B, Kau C C, Manoharan D N, et al. Effects of multi-walled carbon nanotubes on the combustion, performance, and emission characteristics of a single-cylinder diesel engine fueled with palm-oil biodiesel-diesel blend [J]. Energy, 2023, 281: 128350.
[83] Hoseini S S, Najafi G, Ghobadian B, et al. Biodiesels from three feedstock: The effect of graphene oxide (GO) nanoparticles diesel engine parameters fuelled with biodiesel [J]. Renewable Energy, 2020, 145: 190-201.
[84] Zhang J F, Nazarenko Y, Zhang L, et al. Impacts of a Nanosized Ceria Additive on Diesel Engine Emissions of Particulate and Gaseous Pollutants [J]. Environmental Science & Technology, 2013, 47(22): 13077-13085.
[85] Vigneswaran R, Balasubramanian D, Sastha B D S. Performance, emission and combustion characteristics of unmodified diesel engine with titanium dioxide (TiO2) nano particle along with water-in-diesel emulsion fuel [J]. Fuel, 2021, 285: 119115.
[86] Armas O, García-Contreras R, Ramos Á. Pollutant emissions from New European Driving Cycle with ethanol and butanol diesel blends [J]. Fuel Processing Technology, 2014, 122: 64-71.
[87] Geng L, Bi L, Li Q, et al. Experimental study on spray characteristics, combustion stability, and emission performance of a CRDI diesel engine operated with biodiesel–ethanol blends [J]. Energy Reports, 2021, 7: 904-915.
[88] Pala S R, Vanthala V S P, Sagari J. Influence of graphene oxide nanoparticles dispersed mahua oil biodiesel on diesel engine: performance, combustion, and emission study [J]. Biofuels-Uk, 2023, 14(10): 1027-1036.